Electromagnetic properties of the first 2_1^+ excited states in ^{100,102,104}Ru

J. H. Hirata, S. Salém-Vasconcelos, M. J. Bechara, L. C. Gomes, and O. Dietzsch
Instituto de Física, Universidade de São Paulo, Caixa Postal 66318, São Paulo, SP 05315-970, Brazil

(Received 2 July 1997)

Measurements of Coulomb excitation probabilities of the first 2_1^+ state of ^{100,102,104}Ru were carried out using back-scattered ions of ^{4}He and ^{16}O. The static quadrupole moments $Q_{2_1^+}$ and the reduced transition probabilities $B(E2;0_1^+\rightarrow 2_1^+)$ have been determined using the reorientation effect. The quadrupole moments $Q_{2_1^+}$ deduced for the positive sign of the 2_2^+ interference term are -0.54 ± 0.07 eb, -0.64 ± 0.05 eb, -0.62 ± 0.08 eb for ^{100}Ru, ^{102}Ru, and ^{104}Ru, respectively. The reduced transition probabilities $B(E2;0_1^+\rightarrow 2_1^+)$ are 0.493 ± 0.003 e^2b^2, 0.614 ± 0.004 e^2b^2, and 0.809 ± 0.006 e^2b^2, respectively. A compilation of the available experimental results for the reduced eletric quadrupole transition probability $B(E2;0_1^+\rightarrow 2_1^+)$ and for the static quadrupole moments $Q_{2_1^+}$ for the even ruthenium stable isotopes $(96\leqslant A\leqslant 104)$ are presented. [S0556-2813(98)00201-5]

PACS number(s): 25.70.De, 27.60.+j, 21.10.Ky

I. INTRODUCTION

The phenomena of shape coexistence and shape transitions in transitional nuclei such as the ruthenium isotopes have been receiving considerable attention in the past two decades. Because of its symmetry structure, the ''algebraic'' interacting boson approximation (IBA) model is particularly appropriate [1] for treating transitional nuclei. The Ru isotopes, in particular, have recently been investigated within the IBA1 model by Frank [2,3] where an SO(5) dynamical symmetry Hamiltonian with fixed parameters was used. A geometrical interpretation [4] of those results revealed a transition from spherical shape (^{96,98}Ru) to a γ-unstable structure for the higher mass isotopes ($^{100-108}$Ru).

The ''geometrical'' general collective model (GCM) has also been recently applied to the Ru isotopes by Troltenier *et al.* [5] and a spherical structure with a tendency to triaxiality has been obtained. A spherical-triaxial transition for $^{98-108}$Ru with a prolate onset for ^{96}Ru is indicated, in contradiction to the results of the IBA calculation [4]. Common features, e.g., the spherical shape for ^{98}Ru and the β deformation of 0.3–0.4 for the heavier isotopes, are nevertheless obtained in both studies. Phenomenological models such as GCM, use experimental data (excitation energies, electromagnetic matrix elements) to generate an adjusted collective Hamiltonian in a least-squares-fit procedure. If not enough data are available, this procedure can lead to difficulties in the theoretical interpretation [5].

A wealth of new information now exists on the level structure either of neutron-rich Ru isotopes ($A=108-114$) obtained mainly with large γ-detector arrays observing prompt γ decay in spontaneous fission fragments of ^{252}Cf [6,7] or ^{248}Cm [8], and from radioactive decay of proton induced fission products [9] or on the properties of high-lying states in the stable isotopes obtained from incomplete fusion reactions [10]. Those data provide a large set for comparison with model predictions and will most certainly prompt a reinvestigation of the phenomena presented by nuclei in this mass region.

The fact that transition probabilities are a very sensitive tool for the investigation of nuclear properties also makes the availability of precise transition data (even for the low-lying states of the stable isotopes, $96\leqslant A\leqslant 104$) highly desirable for such an analysis. We report here an experimental determination of $B(E2;0_1^+\rightarrow 2_1^+)$ and $Q_{21}{}^+$ for ^{100,102,104}Ru using the reorientation effect [11]. Preliminary results of this study [12] have been reported previously [13], and an investigation of the nuclear form factor in the scattering of α particles on ^{100,102,104}Ru at energies in the vicinity of the Coulomb barrier is the subject of another study [14]. We also present here a compilation of the available experimental information on $B(E2;0_1^+\rightarrow 2_1^+)$ and $Q_{2_1^+}$ values [15–29] for the even ruthenium stable isotopes $(96\leqslant A\leqslant 104)$. A comparison with theoretical model predictions is also made.

II. EXPERIMENTAL PROCEDURE

The experimental method and procedures for data reduction are similar to those used in previous works [30–32] and will not be described in detail here. Targets of ^{100}Ru, ^{102}Ru, and ^{104}Ru were bombarded with ^{4}He and ^{16}O ions from the ''tandem'' electrostatic accelerator at the University of São Paulo. The targets consisted of thin layers ($\sim$5 μg/cm^2 thick for ^{16}O and $\sim$15 μg/cm^2 thick for ^{4}He) of metallic ruthenium enriched in isotopes of masses 100(97.2%), 102(99.35%), or 104(96.35%) evaporated [33] onto $\sim$15 μg/cm^2 thick carbon backings.

The scattered ions were detected in cooled silicon surface barrier detectors of 100 μm depletion depth placed at backward angles. At the most backward scattering angle ($\theta_{lab}\approx 174°$), an annular detector with an 8 mm diameter hole was used. Standard techniques [33,12] were applied to achieve good energy resolution and to minimize the background in the spectra.

Typical spectra are shown in Fig. 1 together with the fit used in the analysis of the data. Resolutions full width at half maximum (FWHM) of $\sim$30 keV for ^{4}He and $\sim$120 keV for ^{16}O were obtained. The elastic and inelastic peaks were well resolved in all heavy-ion spectra, which usually displayed a

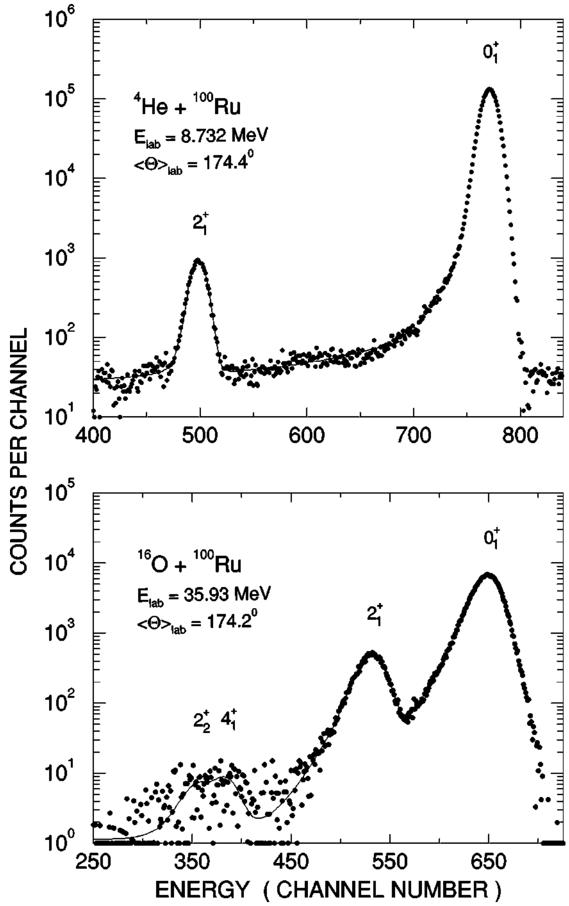

FIG. 1. Spectra of ^{16}O ions and α particles backscattered from ^{100}Ru. The curves through the experimental points are fits to the spectra from which the contributions of scattering from contaminants have been subtracted.

high ratio (~20:1) between the inelastic peak height and the valley between peaks.

The excitation probabilities defined as the ratio of the inelastic to the elastic cross sections $R_{exp}=(d\sigma/d\Omega)_{lab}^{2_1^+}/(d\sigma/d\Omega)_{lab}^{0_1^+}$ were extracted from the spectra using the methods and line fitting programs described in Ref. [34]. The elastic and inelastic contributions of the other Ru isotopes were subtracted from the spectra using the shape of the elastic peak of the main isotope and the supplier assay (Oak Ridge National Laboratory, Isotopes Division) of the target material. Small contributions from Mo isotopes in natural concentration (from impurities present in the W crucible used in the target preparation) were also subtracted. The search for contaminants was made through a careful comparison of ^{4}He and ^{16}O spectra taken with the same target. Particle induced x-ray emission (PIXE) methods were also used with many of the targets in determining elemental impurity concentration [33]. As in other works of this group [35–38], observation of elastically scattered particles with a position sensitive proportional detector [39] located at the focal plane of a high-resolution magnetic spectrograph was also employed in examining the purity of some of the targets.

Statistical plus fitting uncertainties in the evaluation of R_{exp} are of the order of 1% for most of the data taken with the annular detector. Larger uncertainties in R_{exp} are present

TABLE I. Summary of the experimental excitation probabilities (R_{exp}) and associated errors (in percent).

Isotope	Projectile	E_{lab} (MeV)	Θ_{lab}	R_{exp} $\times 10^{-3}$	Error %
100	^{4}He	7.987	174.4	4.27	1.1
		8.236	174.4	5.07	1.0
		8.485	174.4	5.80	0.9
		8.732	174.4	6.71	1.0
	^{16}O	34.95	174.2	62.9	1.0
			130.0	54.0	3.7
			110.0	43.0	3.5
		35.45	174.2	68.1	0.9
			110.0	48.0	3.1
		35.93	174.2	72.7	0.9
			130.0	60.0	3.8
			110.0	51.0	3.0
		36.44	174.2	76.5	0.9
			110.0	55.0	3.0
		36.93	174.2	84.5	0.8
			130.0	70.0	3.2
			110.0	57.0	3.0
102	^{4}He	8.234	173.4	7.43	1.0
			150.0	6.9	1.4
		8.484	173.4	8.51	1.0
			150.0	7.7	1.5
		8.733	173.4	9.7	1.1
			150.0	8.4	2.1
		8.982	173.4	11.0	1.0
			150.0	10.2	1.4
	^{16}O	37.17	173.6	126.0	0.9
		37.41	173.6	127.0	0.9
		37.92	173.6	132.0	0.9
		38.16	173.6	142.0	0.8
		38.90	173.6	149.0	0.9
104	^{4}He	7.736	150.0	8.7	1.3
		7.987	172.8	11.4	1.1
			150.0	10.3	1.3
		8.234	172.8	13.2	1.0
			150.0	11.5	1.3
		8.485	172.8	14.6	1.0
			150.0	13.2	1.3
	^{16}O	37.68	173.4	234.0	1.1
		37.92	173.4	239.0	1.2
		38.17	173.4	250.0	1.0
		38.42	173.4	256.0	1.1
		38.68	173.4	261.0	1.1
		38.93	173.4	263.0	1.2

in the data taken with the smaller solid angle detectors at the other backward angles. The results of this analysis for the experimental excitation probabilities are shown in Table I (together with the corresponding uncertainties), for the different projectiles, bombarding energies, and laboratory scattering angles that were employed.

The validity of the analysis is based on the assumption that the contribution to the 2_1^+ intensity from sources other than pure Coulomb excitation is negligible. The data used in

TABLE II. Level energy, spin and parity, and reduced $E2$ matrix elements (in eb) used in the multiple Coulomb excitation calculation for ^{100}Ru.

Level	I^π	Energy (MeV)	1	2	3	4	5
1	0_1^+	0.0	0.0	M_{12}	0.0	0.0	-0.143
2	2_1^+	0.5396	M_{12}	M_{22}	-0.309	-1.140	-0.663
3	0_2^+	1.1306	0.0	-0.309	0.0	0.0	0.0
4	4_1^+	1.2265	0.0	-1.140	0.0	0.0	0.0
5	2_2^+	1.3621	-0.143	-0.663	0.0	0.0	0.0

TABLE IV. Level energy, spin and parity, and reduced $E2$ matrix elements (in eb) used in the multiple Coulomb excitation calculation for ^{104}Ru.

Level	I^π	Energy (MeV)	1	2	3	4	5
1	0_1^+	0.0	0.0	M_{12}	0.0	-0.183	0.0
2	2_1^+	0.3579	M_{12}	M_{22}	-1.468	-0.914	-0.269
3	4_1^+	0.8885	0.0	-1.468	0.0	0.0	0.0
4	2_2^+	0.8930	-0.183	-0.914	0.0	0.0	0.0
5	0_2^+	0.9880	0.0	-0.269	0.0	0.0	0.0

the present analysis (Table I) were taken at bombarding energies below ‘‘safe values’’ (9.5 MeV for α particles and 38.9 MeV for the ^{16}O beam) obtained using the criterion that half the distance of closest approach in a headon collision must be greater than or equal to the sum of the two nuclei radii [$1.25(A_1^{1/3}+A_2^{1/3})$], plus 6.0 fm. It is estimated [32] that for energies below these values the nuclear contribution should be less than 2%.

The determination of the $B(E2;0_1^+\rightarrow 2_1^+)$ and $Q_{2_1^+}$ values was accomplished by comparing the measured ratios ($R_{\rm exp}$) with the results of a semiclassical coupled channels calculation ($R_{\rm comp}$) for multiple Coulomb excitation (MCE) [40]. The first five levels in ^{100}Ru, ^{102}Ru, and ^{104}Ru, respectively, were used in the calculation. Their excitation energies, J^π values, and the associated electric quadrupole matrix elements $M_{ij}=\langle I_j\|M(E2)\|I_i\rangle$, obtained from the measured $B(E2)$ values and branching ratios (Ref. [20]) are given in Tables II, III, and IV, for ^{100}Ru, ^{102}Ru, and ^{104}Ru, respectively.

The quadrupole matrix elements $M_{12}=[B(E2;0_1^+\rightarrow 2_1^+)]^{1/2}$ and $M_{22}=-1.319Q_{2_1^+}$ were treated as free parameters in a least-squares analysis of the data, after expressing $R_{\rm comp}$ in a functional form given by [34,30]:

$$R^i_{\rm comp}(M_{12},M_{22})=\alpha_i M_{12}^2+\beta_i M_{12}^2 M_{22}+\gamma_i M_{12}^3,$$

where the index i refers to the experimental parameters of $R^i_{\rm exp}$ to which the computed ratio shall be compared. This expression reproduces within less than 0.06% the MCE calculations over our range of M_{12} and M_{22} values. The coefficients α_i, β_i, and γ_i were determined from $R_{\rm comp}$ calculated for given values of M_{12} and M_{22}.

The dependence of $B(E2;0_1^+\rightarrow 2_1^+)$ and $Q_{2_1^+}$ values on the matrix elements $M_{ij}(E2)$ used in the MCE calculation

TABLE III. Level energy, spin and parity, and reduced $E2$ matrix elements (in eb) used in the multiple Coulomb excitation calculation for ^{102}Ru.

Level	I^π	Energy (MeV)	1	2	3	4	5
1	0_1^+	0.0	0.0	M_{12}	0.0	-0.145	0.0
2	2_1^+	0.4750	M_{12}	M_{22}	-0.315	-0.765	-0.138
3	0_2^+	0.9435	0.0	-0.315	0.0	0.0	0.0
4	2_2^+	1.1031	-0.145	-0.765	0.0	0.0	0.0
5	4_1^+	1.1062	0.0	-1.380	0.0	0.0	0.0

has been investigated. This has been done by varying the matrix elements listed in Tables II, III, and IV by 50%. The largest change in $B(E2;0_1^+\rightarrow 2_1^+)$ was of 0.29% due to the $M_{2^+2^{+\prime}}$ matrix element. All the others changes were $\sim$0.05%. The largest change in $Q_{2_1^+}$ due to the matrix elements variations was $\sim$10%.

It is a well-known fact that the computed excitation probability is sensitive to the sign of the second order interference term $M_{12}M_{2s}M_{1s}$ arising from the direct excitation of the first 2_1^+ level and the excitation through a higher lying intermediate 2^+ state s. For ^{100,102,104}Ru, there is one such prominent 2_2^+ state, the 2^+ member of the (0_2^+, 2_2^+, 4_1^+) triplet at about twice the energy of the first 2_1^+ state. Therefore, the values of $B(E2;0_1^+\rightarrow 2_1^+)$ and $Q_{2_1^+}$ were computed for both signs of the matrix elements product $M_{12}M_{1s}M_{2s}$, where $s=5$ for ^{100}Ru (see Table II), and $s=4$ for ^{102,104}Ru (see Tables III and IV).

The $B(E2;0_1^+\rightarrow 2_1^+)$ values obtained in the present work include small corrections for the effects of atomic screening [41] and vacuum polarization [42]. Corrections arising from the semiclassical approximation have also been taken into account, but no corrections have been made for effects of excitation modes other than $\lambda=2$. The $Q_{2_1^+}$ values are strongly affected by the sign of the product $M_{12}M_{1s}M_{2s}$, whereas that of $B(E2;0_1^+\rightarrow 2_1^+)$ shows essentially no dependence on it. The quoted errors have been calculated from a quadratic combination of statistical uncertainties with errors in spectra fitting, incident energy, scattering angle, and in the adopted values for the matrix elements $M_{ij}(E2)$.

The results of the analysis are presented in Fig. 2, where the ratio $R_{\rm exp}/R_{\rm comp}(Q=0)$ (computed in this case for positive interference terms only) has been plotted against the sensitivity parameter ϱ defined [11] by

$$R_{\rm comp}(Q)=R_{\rm comp}(Q=0)(1+\varrho Q),$$

where $R_{\rm comp}(Q=0)$ is the computed excitation probability for $Q=0$. In the MCE calculation of $R_{\rm comp}(Q)$ and $R_{\rm comp}(Q=0)$, the values of $B(E2;0_1^+\rightarrow 2_1^+)$ determined in the present work were used.

III. RESULTS AND DISCUSSION

In Tables V and VI experimental results of other authors on $B(E2;0_1^+\rightarrow 2_1^+)$ and $Q_{2_1^+}$ for ^{96,98,100,102,104}Ru are also presented, together with the results of the present work. The weighted average of all experimental results for

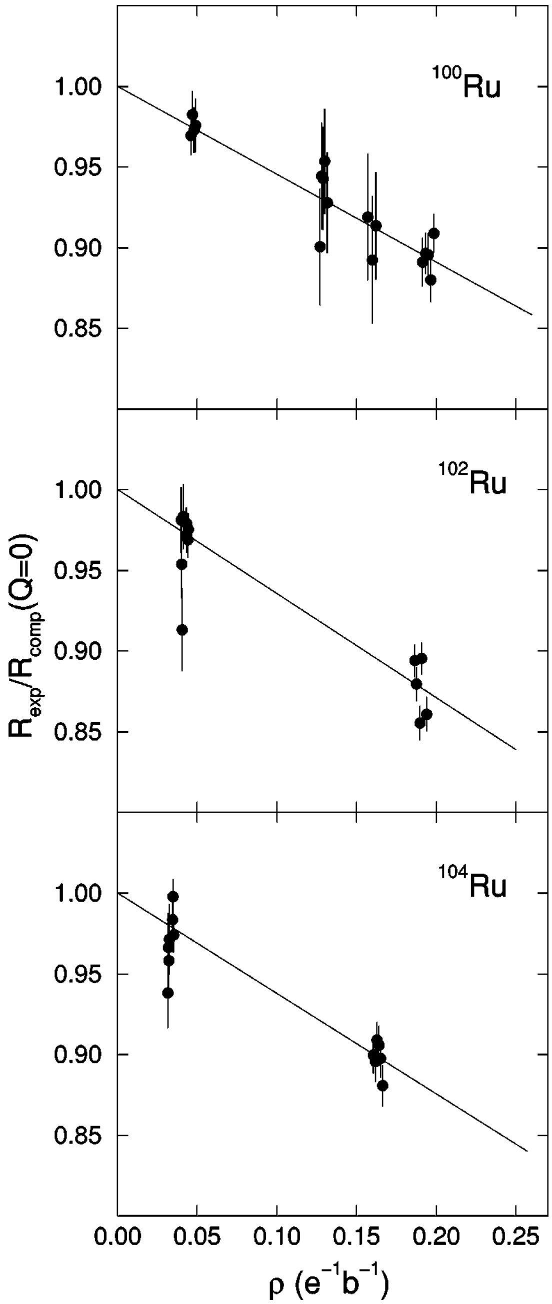

FIG. 2. The ratio $R_{\rm exp}/R_{\rm comp}(Q=0)$ as a function of the sensitivity parameter ϱ, calculated for the positive sign of the interference term $M_{12}M_{1s}M_{2s}$ (see text). The lines are fits to the data using the values of $B(E2;0_1^+\rightarrow 2_1^+)$ obtained in the present work.

$B(E2;0_1^+\rightarrow 2_1^+)$ (present results and results from Refs. [20–25]) and for $Q_{2_1^+}$ (present results and results from Refs. [20–22,26–29]) are also presented. Only relative values for $Q_{2_1^+}$ were determined in Ref. [26]. In Table VI the results of Ref. [26] were normalized to the average value of $Q_{2_1^+}$ for ^{102}Ru obtained by combining the result of the present work with those of Refs. [20,21,27,28]. The renormalized values from Ref. [26] for $Q_{2_1^+}$ for ^{96,98,100,104}Ru presented in column 10 of Table VI were included in the calculation of the average $Q_{2_1^+}$ value for those four isotopes. The average values for all isotopes are presented in column 11 of Table VI. In comparing the average values of Tables V and VI with those of Ref. [19] one should note that in their compilation the authors of Ref. [19] used weighing values that are inversely proportional to the quoted uncertainty rather than inversely proportional to the square of the quoted uncertainty as adopted in the present work. The reduced transition probabilities $[B(E2;0_1^+\rightarrow 2_1^+)]$ and the static quadrupole moments $(Q_{2_1^+})$ values obtained in the present work are in good agreement with the values of Refs. [20] and [21] which were also determined using the reorientation effect in Coulomb excitation with uncertainities comparable to those of the present work.

Figure 3 displays the available information on $B(E2;0_1^+\rightarrow 2_1^+)$ (from the present work and Refs. [20–25]) for the even ruthenium isotopes with $96\leqslant A\leqslant 104$ together with results of theoretical calculations (Refs. [43–45]). In Fig. 4, the experimental $Q_{2_1^+}$ values determined for the constructive interference term $M_{12}M_{1s}M_{2s}$ (from the present work and Refs. [20–22,26–29]) are compared with model predictions (Refs. [5,43,44]) for the even ruthenium isotopes with mass numbers $96\leqslant A\leqslant 104$.

The ruthenium isotopes have been subjected to a variety of theoretical model analysis and in most of these studies they have been examined within the framework of the interacting boson model (IBM) [47] and its extensions. In the IBM, valence nucleon pairs are treated as bosons, and in the

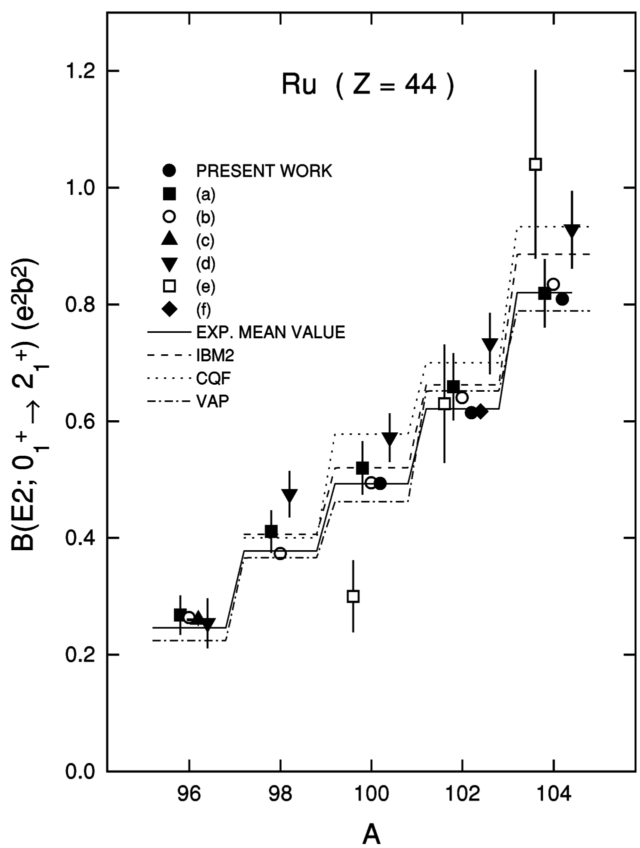

FIG. 3. $B(E2;0_1^+\rightarrow 2_1^+)$ experimental values for the even mass ruthenium isotopes compared to model predictions. The experimental data are from the following: (a) Ref. [23], (b) Ref. [20], (c) Ref. [22], (d) Ref. [24], (e) Ref. [25], (f) Ref. [21]; the experimental average values (see text) are shown as a full line. The model predictions are from IBM2 (dashed line) Ref. [43], CQF (dotted line) Ref. [45] and VAP formalism (dashed-dotted line) Ref. [44] (see text).

TABLE V. $B(E2;0_1^+\rightarrow 2_1^+)$ values in units of $e^2\mathrm{b}^2$ obtained in the present work and from other experiments.

Isotope	Sign [a]	Present work [b]	Ref. [20] [b]	Ref. [20] [c]	Ref. [21] [b]	Ref. [22] [b]	Ref. [23] [b]	Ref. [24] [c]	Ref. [25] [c]	Average value
96			0.236(7)	0.266(26)		0.26(1)	0.268(32)	0.254(41)		0.246(6)
98	+		0.373(7)	0.389(31)			0.411(35)	0.475(38)		0.378(11)
	-		0.372(7)							0.372(7)
100	+	0.493(3)	0.494(6)	0.482(26)			0.520(44)	0.572(40)	0.30(6)	0.493(5)
	-	0.493(3)	0.492(6)							0.493(3)
102	+	0.614(4)	0.640(6)	0.651(35)	0.617(5)		0.659(56)	0.733(51)	0.63(10)	0.621(4)
	-	0.613(4)	0.640(6)							0.621(12)
104	+	0.809(6)	0.834(7)	0.834(44)			0.819(57)	0.928(65)	1.04(16)	0.820(7)
	-	0.805(6)	0.835(7)							0.818(15)

[a]Sign of the interference term $\langle 0_1^+ \| ME2 \| 2_2^+\rangle\langle 2_2^+ \| ME2 \| 2_1^+\rangle\langle 2_1^+ \| ME2 \| 0_1^+\rangle$.
[b]Values obtained from reorientation effect measurements in Coulomb excitation, with detection of inelastically scattered particles.
[c]Values obtained from Coulomb excitation measurements with detection of the emitted γ rays.

original version of IBM (IBM1) no distinction is made between neutron and proton bosons. One of the extensions of the IBM is the proton-neutron interacting boson model (IBM2) [48] which distinguishes proton and neutron degrees of freedom. Another development of the IBM1 is the consistent-Q formalism (CQF) [49] based in a simple Hamiltonian with four parameters which can be determined from experimental data. In the CQF Hamiltonian, the quadrupole operator is the same used for the eletromagnetic transitions. There are also theoretical investigations of the even-even ruthenium isotopes based on a microscopic study in which the $B(E2)$ transition probabilities and the Q_2^+ values are calculated by carrying out variation after projection (VAP) formalism in conjunction with the Hartree-Fock-Bogoliubov (HFB) calculations [44]. The Ru isotopes have also been studied within the framework of the general collective model (GCM) [5] which describes the collective low-energies properties of even-even nuclei in terms of quadrupole surface vibrations [50]. The eletromagnetic properties of the even Ru isotopes have also been analyzed in terms of the boson expansion description [46].

In Fig. 3, the experimental $B(E2)$ values (from the present work and from Refs. [20–25]) are compared with IBM2 predictions (dashed line in Fig. 3) [43], with the results of CQF calculations (dotted line) [45], and with the values obtained by carrying out VAP calculations (dashed-dotted line) [44]. Figure 3 shows that the $B(E2)$ values obtained from IBM2 [43] and from CQF [45] calculations are

TABLE VI. $Q_{2_1^+}$ values in units of eb obtained in the present work and from other experiments.

Isotope	Sign [a]	Present work	Ref. [20]	Ref. [22]	Ref. [21]	Ref. [27]	Ref. [28]	Ref. [29]	Ref. [26] [b]	Average value
96			-0.13(9)	-0.15(27)					-0.24(19)	-0.15(8)
98	+		-0.20(9)						-0.23(14)	-0.21(8)
	-		-0.01(9)							-0.01(9)
100	+	-0.54(7)	-0.43(7)	-0.40(12)					-0.36(8)	-0.44(4)
	-	-0.33(7)	-0.20(7)							-0.27(7)
102	+	-0.64(5)	-0.57(7)		-0.68(8)	-1.06(40)	-0.37(24)		-0.63(4)	-0.63(4)
	-	-0.33(4)	-0.35(7)			-0.99(40)	-0.19(24)			-0.34(3)
104	+	-0.62(8)	-0.70(8)	-0.76(19)			-0.84(21)	-0.63(20)	-0.98(7)	-0.78(7)
	-	-0.05(7)	-0.35(8)				-0.53(21)			-0.20(12)

[a]Sign of the interference term $\langle 0_1^+ \| ME2 \| 2_2^+\rangle\langle 2_2^+ \| ME2 \| 2_1^+\rangle\langle 2_1^+ \| ME2 \| 0_1^+\rangle$.
[b]Values from Ref. [26] renormalized to the average value $(-0.63\pm 0.04\ e\mathrm{b})$ of Q_2^+ for ^{102}Ru calculated with data of present work and Refs. [20], [21], [27], and [28].

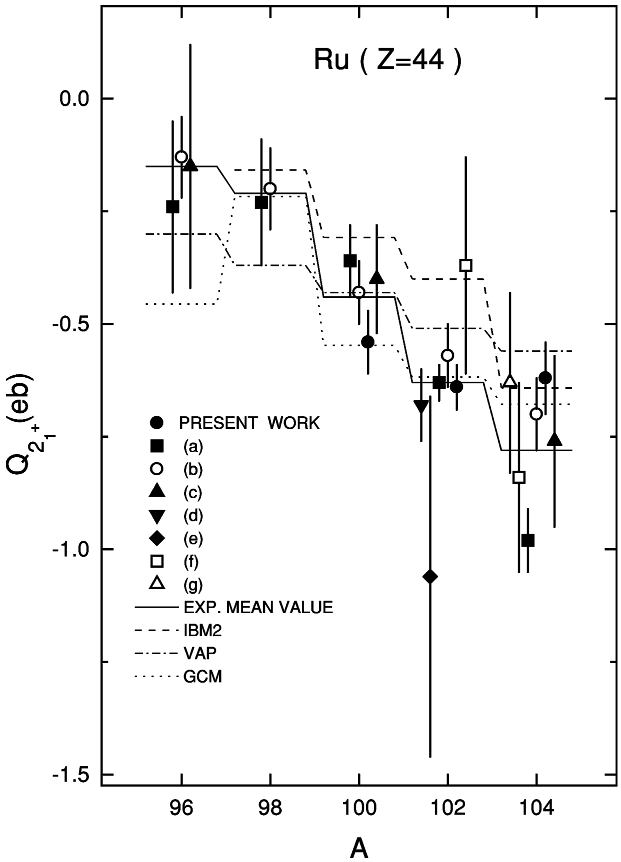

FIG. 4. $Q_{2_1^+}$ experimental values for even mass ruthenium isotopes for constructive interference term (see text) compared with model predictions. The experimental data are from the following: (a) Ref. [26], (b) Ref. [20], (c) Ref. [22], (d) Ref. [21], (e) Ref. [28], (f) Ref. [27], (g) Ref. [29]; the experimental average values (see text) are shown as a full line. The model predictions are from IBM2 (dashed line) Ref. [43], GCM (dotted line) Ref. [5] and VAP formalism (dashed-dotted line) Ref. [44] (see text).

systematically higher than the experimental mean values (full line in Fig. 3) for ^{98,100,102,104}Ru isotopes. However, $B(E2)$ values obtained from another IBM2 study [51] of the even ruthenium isotopes are systematically lower than the experimental mean values for $^{98-104}$Ru. An equally good agreement between the experimental data and the $B(E2)$ values obtained from both IBM2 calculations is observed when relative values only are considered. A visual inspection of this figure also shows that the IBM2 (dashed line) calculations provide a better description of the experimental results when compared to the CQF (dotted line) approach. The $B(E2)$ values calculated in the framework of the IBM1 [52,53] are significantly lower (20–70 %) than the experimental mean values. Figure 3 also shows that the $B(E2)$ values calculated in the VAP formalism are in reasonably good agreement with the experimental results, with values lower than that resulting from the IBM2 and from the CQF calculations. The reduced transition probabilities obtained for ^{98,100,102,104}Ru isotopes from the boson expansion description [46] [$B(E2;2_1^+\rightarrow 0_1^+)=8.1\times 10^{-2}$ e^2b^2; 10.0×10^{-2} e^2b^2; 12.7×10^{-2} e^2b^2; 15.7×10^{-2} e^{2}b^2, respectively] are in good agreement with the experimental results. The tendency of increasing $B(E2)$ values with the neutron number is reproduced by the various models.

In Fig. 4 the experimental quadrupole moment (Q_{21}^+) values for the even Ru isotopes are compared with the IBM2 calculations (dashed line in Fig. 4) [43], with VAP formalism (dotted-dashed line) [44] and with GCM predictions (dotted line) [5] and, in agreement with the experimental results, the Q_{21}^+ values obtained from the various theoretical calculations are negative. Figure 4 shows that the Q_{21}^+ values obtained from the IBM2 [43] are smaller than the average of the experimental quadrupole moments (full line in Fig. 4) for ^{98,100,102,104}Ru isotopes. The Q_{21}^+ values determined in another calculation [51] in the framework of the IBM2 model show a decrease in the absolute value in going from ^{100}Ru ($Q_{21}^+=-0.46$ eb) to ^{102}Ru ($Q_{21}^+=-0.39$ eb). This result is in disagreement with the experimental data that shows an increase in the magnitude of the Q_{21}^+ values with the mass number. The Q_{21}^+ values calculated by employing the VAP formalism increase with the neutron number smoothly than the experimental results and than the other theoretical model predictions. The Q_{21}^+ values obtained from the GCM calculation show a large jump for ^{98}Ru which is not in agreement with the experimental results. The Q_{21}^+ values obtained from the boson expansion description [46] are smaller than the average of the experimental results for ^{100,102,104}Ru isotopes and is higher than the experimental values for ^{98}Ru.

The Q_{21}^+ values calculated from the rigid axial rotor expression $|Q_{21}^+|=0.906|B(E2;0_1^+\rightarrow 2_1^+)|^{1/2}$, using the average of the experimental $B(E2)$ values, are higher than the experimental Q_{21}^+ mean values, ranging from -0.45 eb for $A=96$ to -0.82 eb for $A=104$. The discrepancy between the experimental and the rigid rotor model Q_{21}^+ values decreases with the mass number.

The comparison of the predictions of the various models with the experimental results presented in Figs. 3 and 4 seems to indicate that a better overall agreement is observed between the experimental values for $B(E2)$ and Q_{21}^+ and the results obtained with the variation after projection (VAP) formalism [44] in conjunction with the Hartree-Fock-Bogoliubov ansatz in the mass region investigated in the present work ($A=96$–104). An extension of such a comparison to the neutron-rich isotopes ($A=108$–114) where a large body of experimental data is now available would be useful in explaining the phenomena presented by nuclei in this mass region.

ACKNOWLEDGMENTS

We would like to acknowledge the help of the members of LIP-IFUSP. This work was partially supported by Financiadora de Estudos e Projetos (Finep), Conselho Nacional de Desenvolvimento Científico e Tecnológico (CNPq), and Fundação de Amparo à Pesquisa do Estado de São Paulo (Fapesp).

[1] R. F. Casten and D. D. Warner, Rev. Mod. Phys. **60**, 389 (1988).

[2] A. Frank, P. Van Isacker, and D. D. Warner, Phys. Lett. B **197**, 474 (1987).

[3] A. Frank, Phys. Rev. Lett. **60**, 2099 (1988).

[4] A. Frank, Phys. Rev. C **39**, 652 (1989).

[5] D. Troltenier, J. A. Maruhm, W. Greiner, V. Velazquez Aguilar, P. O. Hess, and J. H. Hamilton, Z. Phys. A **338**, 261 (1991).

[6] Q. H. Lu, K. Butler-Moore, S. J. Zhu, J. H. Hamilton, A. V. Ramayya, V. E. Oberacker, W. C. Ma, B. R. S. Babu, J. K. Deng, J. Kormicki, J. D. Cole, R. Aryaeinejad, Y. X. Dardenne, M. Drigert, L. K. Peker, J. O. Rasmussen, M. A. Stoyer, S. Y. Chu, K. E. Gregorich, I. Y. Lee, M. F. Mohar, J. M. Nitschke, N. R. Johnson, F. K. McGowan, G. M. Ter-Akopian, Yu. Ts. Oganessian, and J. B. Gupta, Phys. Rev. C **52**, 1348 (1995).

[7] K. Butler-Moore, R. Aryaeinejad, J. D. Cole, Y. Dardenne, R. G. Greenwood, J. H. Hamilton, A. V. Ramayya, W. C. Ma, B. R. S. Babu, J. O. Rasmussen, M. A. Stoyer, S. Y. Chu, K. E. Gregorich, M. Mohar, S. Asztalus, S. G. Prussin, K. J. Moody, R. W. Lougheed, and J. F. Wild, Phys. Rev. C **52**, 1339 (1995).

[8] J. A. Shannon, W. R. Phillips, J. L. Durell, B. J. Varley, W. Urban, C. J. Pearson, I. Ahmad, C. J. Lister, L. R. Morss, K. L. Nash, C. W. Williams, N. Schulz, E. Lubkiewicz, and M. Bentaleb, Phys. Lett. B **336**, 136 (1994).

[9] J. Äystö, P. P. Jauho, Z. Janas, A. Jokinen, J. M. Parmonen, H. Pentillä, P. Taskinen, R. Béraud, R. Duffait, A. Emsallem, J. Meyer, M. Meyer, N. Redon, M. E. Leino, K. Eskola, and P. Dendooven, Nucl. Phys. **A515**, 365 (1990).

[10] H. Dejbakhsh and S. Bouttchenko, Phys. Rev. C **52**, 1810 (1995).

[11] J. de Boer and J. Eichler, in *Advances in Nuclear Physics*, edited by M. Baranger and E. Vogt (Plenum, New York, 1968), Vol. 1, p. 1.

[12] J. H. Hirata, PhD Thesis, University of São Paulo, 1984.

[13] J. H. Hirata and O. Dietzsch, in *Proceedings ot the International Conference on Nuclear Physics*, Berkeley, 1980 (unpublished), Vol. 1, p. 102; J. H. Hirata and O. Dietzsch, in *Proceedings of the International Conference on Nuclear Structure*, Amsterdam, 1982, edited by A. Van der Woude and B. J. Verhaar (unpublished), Vol. 1, p. 131.

[14] L. C. Gomes, L. B. H. Matsushigue, T. B. Lewin, J. L. M. Duarte, J. H. Hirata, S. Salém-Vasconcelos, and O. Dietzsch, Phys. Rev. C **54**, 2296 (1996).

[15] P. Raghavan, At. Data Nucl. Data Tables **42**, 189 (1989).

[16] B. Singh and J. A. Szues, Nucl. Data Sheets **60**, 1 (1990).

[17] D. de Frenne and E. Jacobs, Nucl. Data Sheets **63**, 373 (1991).

[18] J. Blachot, Nucl. Data Sheets **64**, 1 (1991).

[19] S. Raman, C. H. Malarkey, W. T. Milner, C. W. Nestor, Jr., and P. H. Stelson, At. Data Nucl. Data Tables **36**, 1 (1987).

[20] S. Landsberger, R. Lecomte, P. Paradis, and S. Monaro, Phys. Rev. C **21**, 588 (1980).

[21] A. Bockisch, M. Miller, A. M. Kleinfeld, A. Gelberg, and U. Kaup, Z. Phys. A **292**, 265 (1979).

[22] C. Fahlander, L. Hasselgren, G. Possnert, and J. E. Thun, Phys. Scr. **18**, 47 (1978).

[23] F. K. McGowan, R. L. Robinson, P. H. Stelson, and W. T. Milner, Nucl. Phys. **A113**, 529 (1968).

[24] P. H. Stelson and F. K. McGowan, Phys. Rev. **110**, 489 (1958).

[25] G. M. Temmer and N. P. Heydenburg, Phys. Rev. **104**, 967 (1956).

[26] M. Maynard, D. C. Palmer, J. R. Cresswell, P. D. Forsyth, I. Hall, and D. G. E. Martin, J. Phys. G **3**, 1735 (1977).

[27] A. Gelberg, B. Herskind, R. Kalish, and M. Neimann, in *International Conference on Hyperfine Interactions Studied in Nuclear Reactions and Decay*, Uppsala, 1974, edited by E. Karlsson and R. Wäppling (unpublished).

[28] M. F. Nolan, I. Hall, D. J. Thomas, and M. J. Throop, J. Phys. A **6**, 57 (1973).

[29] P.H. Stelson (private communication).

[30] M. J. Bechara, O. Dietzsch, M. Samuel, and U. Smilansky, Phys. Rev. C **17**, 628 (1978).

[31] M. J. Bechara, O. Dietzsch, and J. H. Hirata, Phys. Rev. C **29**, 1672 (1984).

[32] S. Salém-Vasconcelos, M. J. Bechara, J. H. Hirata, and O. Dietzsch, Phys. Rev. C **38**, 2439 (1988).

[33] K. Koide, F. C. Sampaio, E. M. Takagui, J. H. Hirata, and O. Dietzsch, Nucl. Instrum. Methods Phys. Res. **215**, 61 (1983).

[34] Z. Berant, R. A. Eisenstein, Y. Horowitz, U. Smilansky, P. N. Tandon, J. S. Greenberg, A. M. Kleinfeld, and H. G. Maggi, Nucl. Phys. **A196**, 312 (1972).

[35] H. Takai, K. Koide, A. Bairrio-Nuevo, Jr., and O. Dietzsch, Phys. Rev. C **38**, 741 (1988).

[36] K. Koide, H. Takai, A. Bairrio-Neuvo, Jr., and O. Dietzsch, Phys. Rev. C **39**, 1636 (1989).

[37] E. M. Takagui, G. R. Satchler, H. Takai, K. Koide, and O. Dietzsch, Nucl. Phys. **A514**, 120 (1990).

[38] S. Salém-Vasconcelos, E. M. Takagui, M. J. Bechara, K. Koide, and O. Dietzsch, Phys. Rev. C **50**, 927 (1994).

[39] K. Koide, A. Bairrio-Nuevo, Jr., H. Takai, B. Marechal, and O. Dietzsch, Nucl. Instrum. Methods Phys. Res. **215**, 177 (1983).

[40] A. Winther and J. de Boer, in *Coulomb Excitation*, edited by K. Alder and A. Winther (Academic, New York, 1966), p. 303.

[41] J. X. Saladin, G. E. Glenn, and R. Pryor, Phys. Rev. **186**, 1241 (1969).

[42] L. L. Foldy and E. Erikson, Phys. Rev. **95**, 1048 (1954).

[43] P. Van Isacker and G. Puddu, Nucl. Phys. **A348**, 125 (1980).

[44] A. Bharti, R. Devi, and S. K. Khosa, J. Phys. G **20**, 1231 (1994).

[45] D. Bucurescu, G. Cata, D. Cutoiu, G. Constantinescu, M. Ivascu, and N. V. Zamfir, Z. Phys. A **324**, 387 (1986).

[46] K. Weeks and T. Tamura, Phys. Rev. C **22**, 888 (1980).

[47] A. Arima and F. Iachello, Ann. Phys. (N.Y.) **99**, 253 (1976).

[48] A. Arima, T. Ohtsuka, F. Iachello, and I. Telmi, Phys. Lett. **66B**, 205 (1977).

[49] D. D. Warner and R. F. Casten, Phys. Rev. C **28**, 1798 (1983).

[50] J. Eisenberg and W. Greiner, in *Nuclear Theory 1: Nuclear Collective Models*, 3rd ed. (North-Holland, Amsterdam, 1987).

[51] A. Giannatiempo, A. Nannini, A. Perejo, P. Sona, and D. Artoiu, Phys. Rev. C **53**, 2969 (1995).

[52] R. F. Casten, W. Frank, and P. Von Bretano, Nucl. Phys. **A444**, 133 (1985).

[53] A. K. Vlasnikov and V. M. Mikhailov, Izv. Akad. Nauk SSSR, Ser. Fiz. **53**, 58 (1989).